International Journal of Fluid Power 14 (2013) No. 3 pp. 5-14

CFD ANALYSIS AND IMPROVEMENT OF TORQUE DETECTED TYPE FLOW METER

Takayoshi Ichiyanagi and Takao Nishiumi

National Defense Academy, Department of Mechanical Systems Engineering, 1-10-20 Hashirimizu, Yokosuka, Kanagawa, JAPAN
ichiyana@nda.ac.jp

Abstract

We propose a unique flow meter that uses a lateral flow force generated on a pressure sensing bar in a rectangular flow channel. The mathematical model, based on laminar viscous flow analysis, has been previously described and the design criterion was established from the fundamental characteristics. The test flow meter has also been investigated experimentally to clarify the torque versus flow characteristics. Although the meter performed well in terms of linearity and repeatability in the low flow rate region, the results deviated from the analytical results at high flow rates. This paper presents a theoretical analysis of the flow meter based on CFD (computational fluid dynamics). The aim is to examine the flow behavior and the pressure distribution inside the meter. CFD analysis is conducted over a range of dimensional configurations and boundary conditions. The flow versus torque characteristics are derived from pressure distribution results and compared with the analytical model. On the basis of CFD analysis, we propose a revised configuration of the flow meter, and verify its performance experimentally.

Keywords: flow meter, CFD analysis, laminar flow, pressure distribution, hydraulic lock

1 Introduction

Understanding the flow conditions in hydraulic systems requires precise and instantaneous flow rate measurements. Therefore various types of flow meter were already developed (e.g. Esser et al., 1994; Yokota et al., 1992; Zhao et al., 1987), and many of the existing flow meters, especially those that measure steady flow rate, are widely used in the industry. Our research group has proposed a new flow-rate-measuring technique for use in hydraulic systems (Nishiumi et al., 2004). The proposed flow meter utilizes the lateral flow force generated in the inclined flow clearance. This force is known to occur if the flow clearance between the sleeve and spool is tapered, similar to certain hydraulic components such as spool type valves. This lateral force frequently causes a hydraulic lock, which is a major problem in hydraulic servovalves (Blackburn, 1953; Geißler, 1998). However, the proposed flow meter exploits this force by marginally sloping the rectangular bar in the flow line to generate torque. The torque generated around the center of the bar is proportional to the force induced by the flow through the channel. Thus, the flow rate can be assessed directly by measuring the torque. In previous works, on the basis of the two-dimensional laminar viscous flow, a mathematical model has been formulated. The design criterion for the proposed flow meter was then established by examining the fundamental characteristics. The torque versus flow characteristics of the flow meter were investigated experimentally. Although the flow meter performed with strong linearity at low flow rates, its performance deviated from its theoretical performance at higher flow rates.

To identify the cause of this deviation, we present a theoretical analysis of the proposed flow meter based on CFD (computational fluid dynamics). CFD analysis enables a detailed investigation of the flow behavior and pressure distribution inside the flow meter. CFD simulations are conducted over a range of boundary conditions and design parameters. From the results, the flow response to the generated torque is derived. The flow rate-torque characteristics are compared with the analytical model by which the flow meter design is evaluated.

Next, the outcomes of the CFD simulations are used to improve the linearity of the meter at high flow rates. The revised flow meter is assessed in a series of experiments. The performance of the revised instrument is evaluated by measuring its static characteristics, such

This manuscript was received on 15 February 2013 and was accepted after revision for publication on 19 July 2013

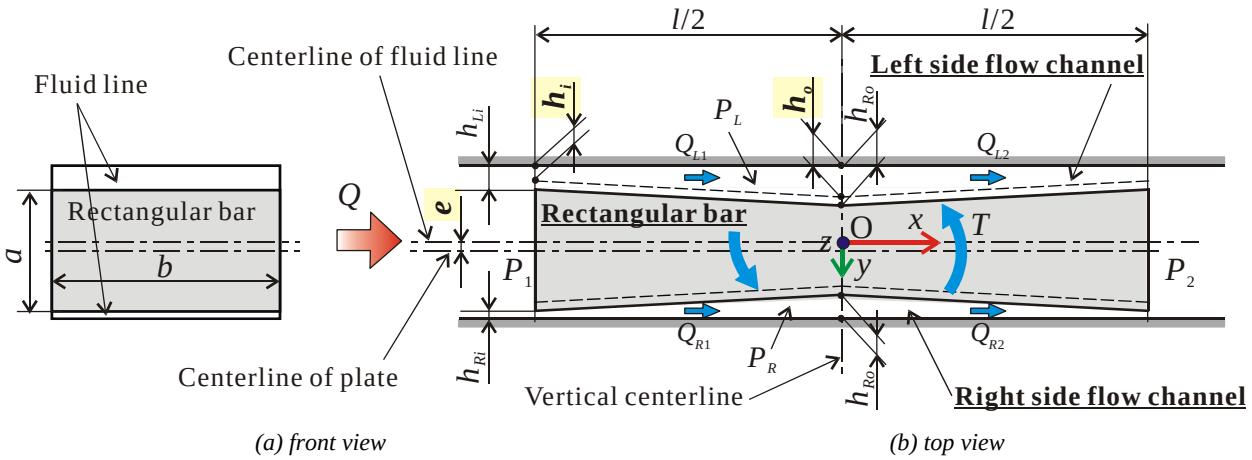

(a) front view *(b) top view*

Fig. 1: *Schematic diagram of proposed flow meter*

as pressure distribution inside the flow meter. Finally, in order to evaluate the practicality of the meter, the quasi-static flow rate measured by the revised flow meter is compared with that of a reference flow meter.

2 Torque Detected Flow Meter

Figure 1 shows the basic structure of the proposed flow meter, viewed from above. The rectangular bar, which slopes minimally toward its center, is placed inside a rectangular channel. Working fluid passes separately through the two flow channels divided by the rectangular bar. The flow becomes a convergent clearance flow between the two planes from the entrance to the vertical centerline, and a divergent clearance flow from the vertical centerline to the exit. Since the centerline of the bar is offset a distance e from the flow centerline, a pressure difference occurs between the upper and lower flow channels. This pressure difference is symmetrically distributed around the bar center O. Therefore, a torque is generated around O. Since the torque is proportional to the flow rate, the latter is obtained directly by measuring the torque.

The theoretical relationship between the flow rate Q and the torque T are expressed by Eq. 1. This analytical model, based on laminar viscous flow analysis, has been formulated in the reference paper (Nishiumi et al., 2004) and is also described in the appendix A.

$$\frac{Q}{T} = \frac{h_i^3}{12\mu\kappa l^3} \tag{1}$$

h_i is the entrance clearance without offset e, l is the length of rectangular bar, and κ is the gain factor, which is defined as the ratio of the flow coefficient ε and non-dimensional torque τ as follows.

$$\kappa = \frac{\varepsilon}{\tau} \tag{2}$$

The flow coefficient ε and non-dimensional torque τ are both a function of the non-dimensional clearance $\bar{h} = h_o / h_i$ (h_o: center clearance without offset e) and the non-dimensional offset $\bar{e} = e / h_i$ (see the appendix A). Therefore the gain factor κ is determined by the dimensions of the flow meter. Equation 1 indicates that the flow rate Q can be obtained by measuring the torque T around the bar center O, since the right side of Eq. 1 becomes constant.

Table 1: Specification of proposed flow meter

Non-dimensional clearance	$\bar{h}$ = 2.36
Non-dimensional off-set	$\bar{e}$ = 0.318 0.5 0.681
Entrance clearance without offset e	h_i = 1.1mm
Length of bar	l = 190mm
Width of bar	a = 22.0mm
Height of bar	b = 34.8mm
Nominal dynamic viscosity of fluid	μ = 0.0280Pa·s

3 CFD Analysis

3.1 Modelling

On the basis of the analytical model explained in the previous chapter, the basic static characteristics of the proposed flow meter are examined for specified dimensions. The specifications used in the CFD analysis are listed in Table 1. These parameters are designated to ensure laminar main flow. Hydraulic oil ISO VG32, with dynamic viscosity μ = 0.0280 Pa·s at 40°C, is used as the working fluid.

The geometric model and a mesh of the proposed flow meter are shown in Fig. 2. In accordance with the experimental setup, the main components are the flow meter and a connecting pipe. The flow meter is divided into the upper cover, the body, and the bar. In Fig. 2, so that the mesh is visible, the upper cover and the section of the body facing the right side of the flow channel are shown as transparent. Circular pipes are connected at the inlet and outlet of the flow meter. These components are included in the CFD analysis but are excluded from the analytical model.

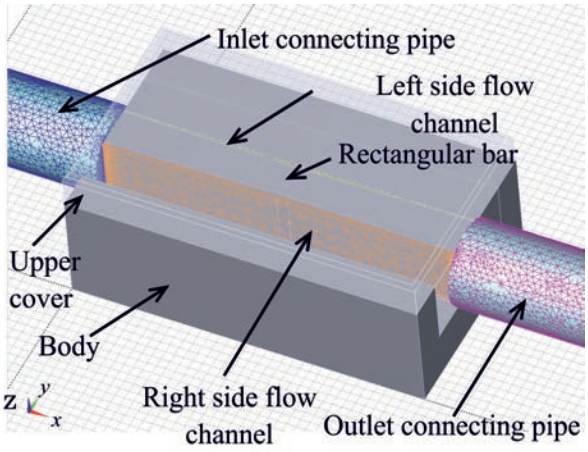

Fig. 2: *Geometric and mesh model*

Appropriate meshing is critical to ensure meaningful results and computational solution convergence. After performing some preliminary simulations, the mesh was refined using a conventional adaptive mesh tool. Hereafter, regions of high pressure and velocity gradients; namely, the inlet and outlet areas of the flow meter, were assigned a higher mesh density.

CFD analysis was conducted using the commercial package STAR-LT, which implements a STAR-CD code. Although a laminar flow is required for the proposed flow meter, the standard k-ε turbulent model is used as the flow condition, in order to investigate local turbulence effects. In this study, the constant flow velocity (denoting the required flow rate at the inlet of the connecting pipe) becomes an inlet boundary condition. Calculations are performed using the SIMPLE algorithm, which yields a fast convergence rate.

3.2 Simulation Results and Considerations

A typical pressure contour plot for Q = 1.0 L/min and the non-dimensional offset $\bar{e}$ = 0.5 is illustrated in Fig. 3. From this figure, the pressure drop is seen to dominate at the flow meter. This pressure drops gradually from the inlet to the outlet of the flow meter in both left and right flow channels. The pressure gradients differ between the left and right flow channels. As mentioned above, this pressure difference produces the torque around the bar center O.

Figure 4 is a pressure contour plot of the flow meter inlet area in the x-y cross-section. The flow rate and the non-dimensional offset are Q = 10.0 L/min and $\bar{e}$ = 0.5, respectively. Clearly, the pressure contour profiles differ between the left and right sides of the flow channel, especially around the flow meter inlet. On the right side, the pressure is distributed constantly in the y direction, as expected. More detailed pressure profiles are shown in Fig. 5. These plots show the pressure contours and flow velocity vectors around the left side of the flow channel inlet at flow rates (a) Q = 1.0 L/min and (b) Q = 10.0 L/min. The analytical model assumes that the velocity in the y direction can be ignored, since it is small as compared to the x velocity. Therefore, the pressure becomes constant in the y cross-sectional area and drops gradually in the downstream x direction. However, Fig. 5 indicates that the assumptions of the analytical model are inappropriate around the inlet of the left-side flow channel, because an abrupt contraction flow develops there. This contraction flow results from the difference in the cross-sectional area between the connecting pipe and flow channel in the flow meter. Consequently, velocity and pressure graduation is developed in the y direction. The influence of this abrupt contraction flow becomes significant at higher flow rates, as shown in Fig. 5(b). Local minimum pressure is found near the edge of the flow meter inlet at Q = 10.0 L/min, while the pressure distribution profile remains close to that predicted by the analytical model at lower flow rates (Q = 1.0 L/min).

Figure 6 shows horizontal pressure distributions in the left and right sides of the flow channel obtained by CFD resutlts. Results are plotted for low (Q = 1.0 L/min) and high (Q = 10.0 L/min) flow rates. It should be noted that these pressures are located at the bar surface. From this figure, it is apparent that the pressure difference induced by a combination of parallel expanse and narrow clearance flow is sufficient to generate a torque around x = 0 mm. This pressure distribution profile changes as the flow rate increases, especially in the left side of the flow channel (P_L), where contraction flow develops. The pressure drop at the inlet (x = - 95 mm) exerts a significant effect on the distribution of pressure difference, and thereby determines the magnitude of the generated torque.

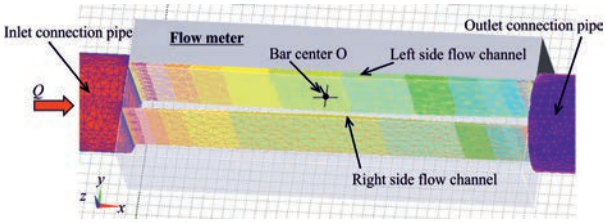

Fig. 3: *Typical pressure contour plot (Q = 1.0L/min, = 0.5)*

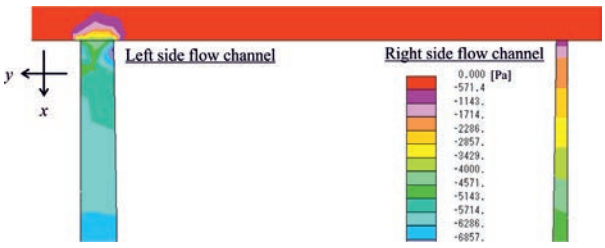

Fig. 4: *Pressure contour plot at inlet of flow meter (Q = 10.0 L/min, = 0.5)*

Figure 7 shows how the increasing flow rate affects the pressure difference between the left and right flow channels. In this figure, the non-dimensional distributions of pressure difference $\Delta\overline{P}$ are plotted for three different flow rates, together with the predictions of Eq. A.6 from Appendix A. Clearly, the abrupt contraction flow at the inlet influences the upstream side of the flow meter. As the flow increases, the numerical solutions deviate more from the analytical results, suggesting that the magnitude of the generated torque similarly deviates with increasing flow. Downstream of the flow meter, CFD simulations are consistent with analytical results at all flow rates.

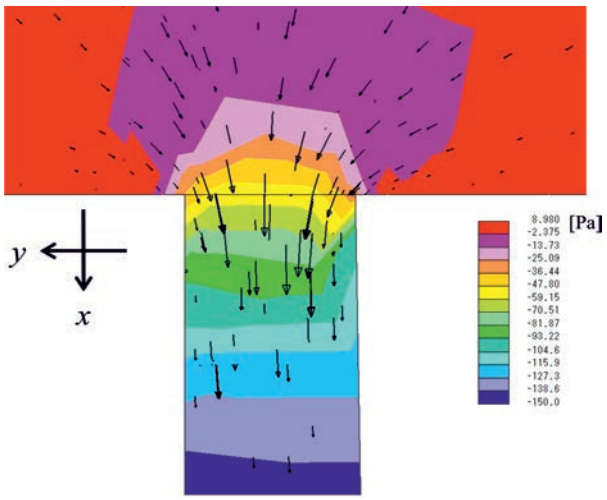

(a) Q = 1.0 L/min

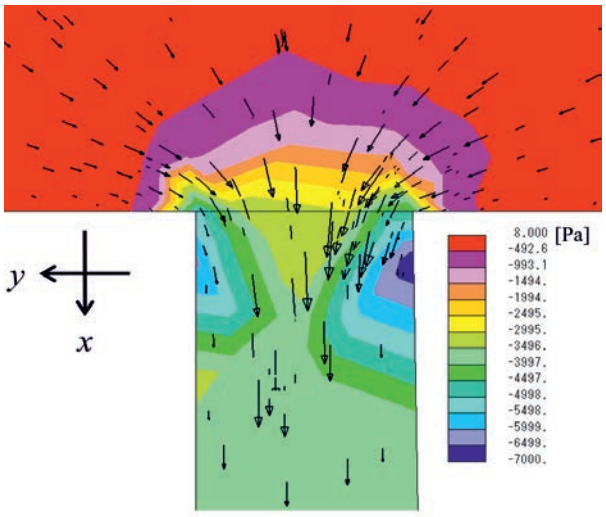

(b) Q = 10.0 L/min

Fig. 5: *Pressure contour (a) and flow velocity vector (b) of left side flow channel inlet ($\bar{e}$ = 0.5)*

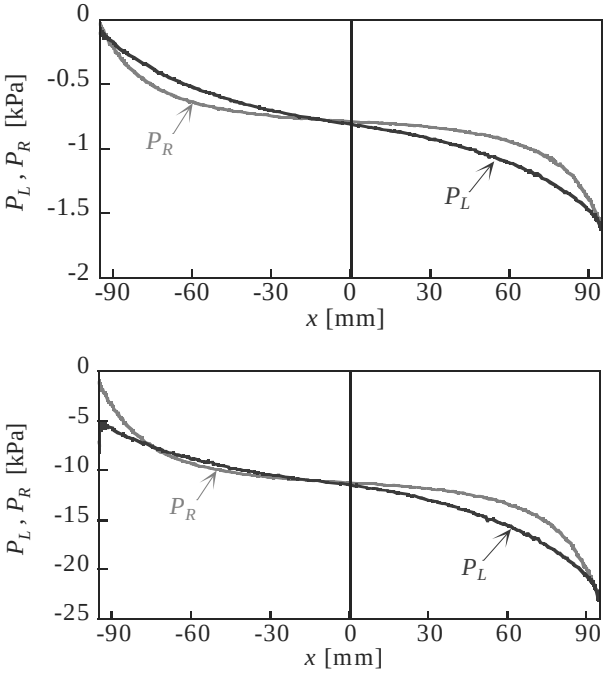

Fig. 6: *Pressure distribution of the upper and lower channels ($\bar{e}$ = 0.5)*

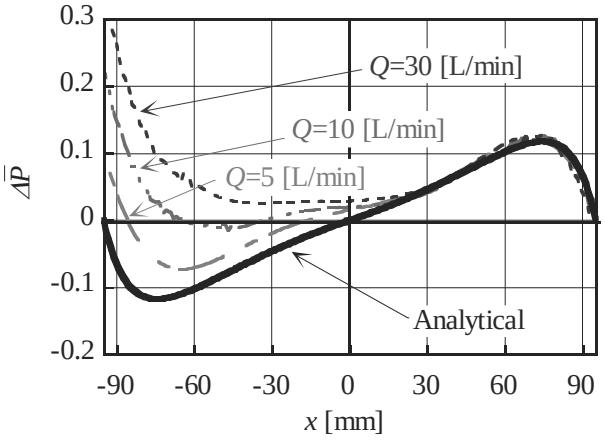

Fig. 7: *Nondimensional pressure difference distribution $\Delta\bar{P}$ ($\bar{e}$ = 0.5)*

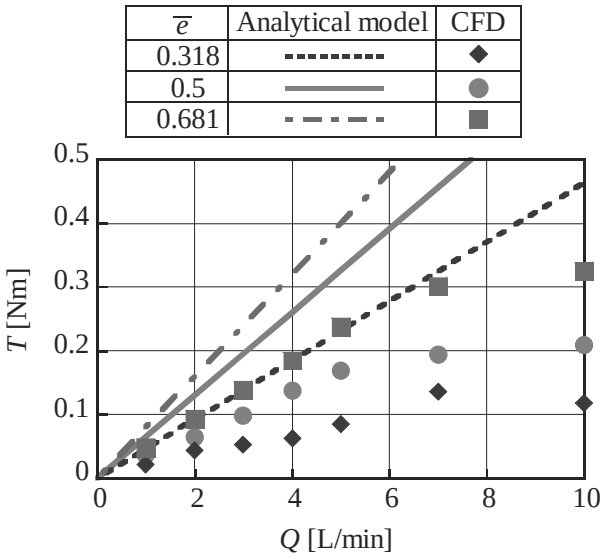

Fig. 8: *Flow rate versus generated torque various values of non-dimensional off-set*

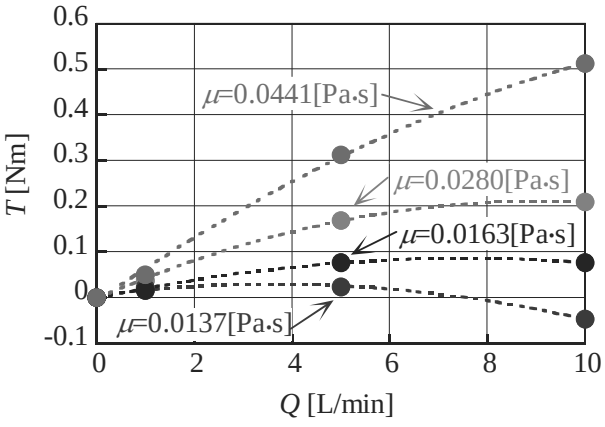

Fig. 9: *Flow rate versus generated torque various values of fluid viscosity ($\bar{e}$ = 0.5)*

The relationship between the flow rate and generated torque is examined in Fig. 8 and 9. Figure 8 compares the CFD simulation results with the analytical predictions obtained from Eq. 1 for three offset conditions ($\bar{e}$ = 0.318, 0.5, 0.681). The slope of the flow rate versus torque plot increases both

numerically and analytically, since the gain factor κ increases with $\bar{e}$; see Fig. A.1. Both sets of results show a similar qualitaive trend as offset is varied. However, as evidenced in Fig. 7, CFD results are roughly 60 % of their analytical counterparts in regions of small flow rate Q < 5.0 L/min, and deviate further as the flow rate increases. Consequently, when the torque generated by the abrupt contraction flow at the inlet exceeds that generated at the downstream side, the overall torque becomes negative; thus, resulting in a clockwise rotation. Figure 9 plots the flow rate Q versus the generated torque T for the non-dimensional offset $\bar{e}$ = 0.5 at different fluid viscosity μ, which is another crucial parameter of the proposed flow meter; see Eq. 1. From this figure, the gain is seen to be exactly proportional to the fluid viscosity. Therefore, for practical use, gain in the flow rate with respect to generated torque can be calibrated by measuring the fluid temperature as an indicator of fluid viscosity. This idea will be discussed in the following section.

4 Experimental Considerations

4.1 Revised Flow Meter

In Section 3, it was found that abrupt contraction flow developed at the inlet destroys the linearity between the flow rate and generated torque. Therefore, we seek ways of preventing this flow. To this end, an inlet block was inserted upstream of the rectangular bar to provide an entrance region for both left and right flow channels. The abrupt contraction flow from the circular connecting pipe now appears at the entrance of the inlet block, rather than at the torque-sensing rectangular bar. The configuration of the revised flow meter is shown in Fig. 10. To reduce the influence of abrupt expanse flow at the bar outlet, a second block is positioned behind the rectangular bar. Because these two blocks must fit within the flow meter body, the rectangular bar must be shortened by almost one third. Equation 1 shows that the ratio of the flow rate to the generated torque is proportional to the inverse cube of the bar length.

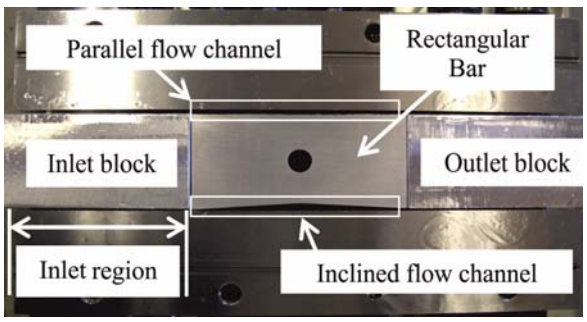

Fig. 10: *Revised configuration of test flow meter*

Thus, the gain factor of the flow rate and the generated torque must be adjusted to approximately equal the original bar length, if the same torque meter is used. This is achieved by rearranging the configuration of the flow channel. The left flow channel is set to parallel by specifying a bar with “one side is flat/another is sloped minimally toward the center.” The combination of these flow channels increases the gain factor κ in Eq. 1. The analytical model of the revised flow meter is similar to that of Section 2, and is described in Appendix B.

4.2 Experimental Apparatus

Figure 11 shows the experimental apparatus used to verify the static characteristics of the test flow meter. The hydraulic circuit comprises a variable displacement pump, filter, test flow meter, load valve, a reference flow meter, heat exchanger and oil tank. Line pressure is regulated by the pressure compensator of the pump and the flow rate through the test flow meter is adjusted manually by the load valve. This flow rate is measured by the reference flow meter (type: external gear; measuring range: 0.6 - 63 L/min). The torque transducer (type: strain gage; rated torque: T_{max} = 0.5 Nm; resolution: 1 / 3000 F.S.) used in this study measures non-rotating torques. The transducer is fixed within the test flow meter and its shaft (operating as a torsion bar) is directly connected to the rectangular bar, as shown in Fig. 12. Because the shaft is highly rigid, its angular displacement is minimal, ensuring that the connected rectangular bar is scarcely rotated. To investigate the pressure distribution in each flow channel, conduits are provided to the left and right sides of the test flow meter. Pressure distribution is measured by a differential pressure transducer (type: strain gage; rated differential pressure: 20 kPa). Interval lengths of the conduits are 30 mm (No. 0 - 1, No. 8 - 9), 18.5 mm (No. 3 - 4, No. 5 - 6), 23 mm (No. 4 - 5), 25 mm (other). One port of the differential pressure transducer is always connected to conduit No. 0 (inlet of flow meter) and another port is connected to conduits No. 1 to No. 9 sequentially. In this manner, the pressure difference at the inlet of the test flow meter is assessed. Viscosity of the oil is estimated from temperature measured by a thermocouple. All measurements are stored in a PC via a data acquisition system containing a 16-bit AD converter.

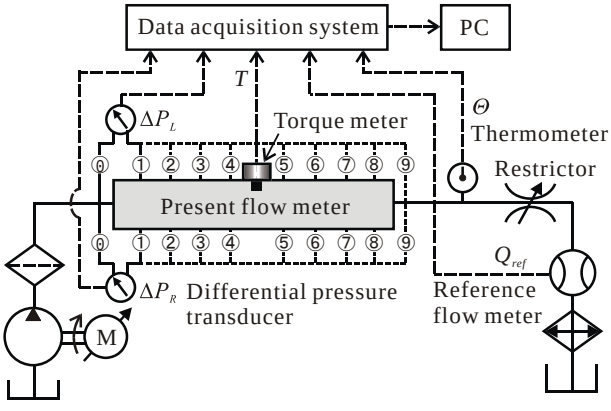

Fig. 11: *Measurement system*

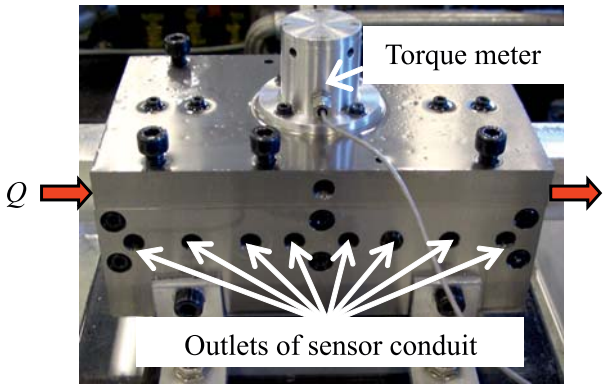

Fig. 12: *Test flow meter*

4.3 Experimental Results

The effect of the inserted blocks is displayed in Fig. 13. This figure plots flow rate Q_{ref} measured by the reference flow meter as a function of detected torque T at oil temperature Θ = 40°C (μ = 0.0280 Pa·s). Clearly, the blocks improve the linearity of the flow–torque gain characteristics. As explained in the previous section, without the entrance region the linearity is retained only up to Q_{ref} = 2.0 L/min and the detected torque saturates as flow rate increases.

From Eq. 1, it is noted that the flow–torque gain characteristic of the proposed flow meter depends on the fluid viscosity μ. This relationship is shown in Fig. 14. The reference flow rate Q_{ref} versus detected torque T is plotted in Fig. 14 as oil temperature rises from Θ = 30°C to 50°C, corresponding to μ = 0.0441 - 0.0188 Pa·s. For all of the tested viscosities, high linearity up to the rated torque is achieved. Similarly excellent results were acquired in repeat experiments. In Table 2, the experimentally-derived gain factor κ_{ex} is compared with the analytical gain factor κ_r under changing viscosity. The ratio of experimental to analytical gain factor is around 0.785 ~ 0.835, implying that the flow-torque gain shown in Fig. 14 virtually depends on the viscosity alone. Hence, in practice, the proposed flow meter can be calibrated by monitoring the fluid viscosity via fluid temperature measurements. It should be noted that the pressure dependent characteristics of the fluid viscosity must be also taking into account if the working pressure is extremely high.

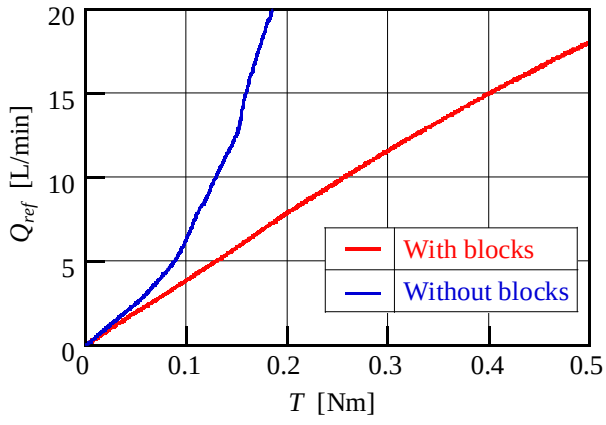

Fig. 13: *Effect of inlet and outlet block (μ = 0.0280 Pa·s)*

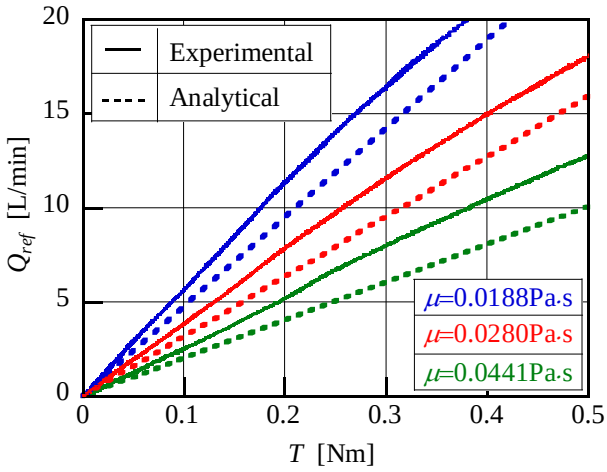

Fig. 14: *Basic static characteristics*

Table 2: Ratio of experimental and analytical gain factor

Dynamic viscosity μ [Pa·s]	Temperature Θ [°C]	κ_{ex}/κ_r
0.0188	50	0.835
0.0227	45	0.813
0.0280	40	0.833
0.0346	35	0.787
0.0441	30	0.785

Figure 15 shows the pressure distribution in the left and right flow channels at the reference flow rate Q_{ref} = 4.0 L/min under the condition of fluid viscosity μ = 0.0441 Pa·s.

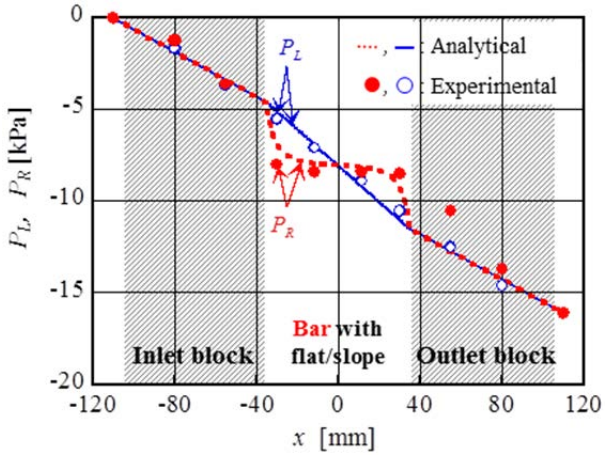

Fig. 15: *Pressure distribution of revised flow meter (Q_{ref} = 4L/min, μ = 0.0441Pa·s)*

The experimental and analytical results are shown as points and lines, respectively. The flow channels of the inlet and outlet blocks, as well as the left flow channel of the bar, are parallel clearances, while the right bar channel is an inclined clearance. The experimental pressure distributions in the left and right sides of the bar are consistent with the predictions of a two-dimensional laminar viscous flow. This figure also suggests that the torque around the rectangular bar center results from the pressure differences between the parallel and inclined clearance.

4.4 Evaluation as Flow Meter

In this section, the practicality of the proposed meter is assessed by investigating its flow rate (obtained from the measured torque and the oil temperature). Flow rate calculations are processed on-line by a digital signal processor embedded in the data acquisition system. In this study, the fluid viscosity is related to the measured temperature by the following equation, based on Walther equation (ASTM, 1992).

$$\mu(\Theta) = -6.09\times10^{-4} + 8.70\times10^{-4} \times \exp\left\{\frac{6.72\times10^{9}}{(\Theta+273)^{3.72}}\right\} \quad (3)$$

Then the flow rate of the proposed flow meter now becomes the following equation from Eq. 1.

$$Q(T,\Theta) = C_1 \frac{T}{\mu(\Theta)} \quad (4)$$

Here, C_1 is a constant value expressed by the Eq. 5.

$$C_1 = \frac{h_i^3}{C_2 \kappa_r l^3} \quad (5)$$

To account for the deviation between the experimental and analytical gain factor, the avarage value of the ratio of experimental to analytical gain factor (κ_{ex}/κ_t) is used as a correction coefficient C_2, derived from the experimental results of Table 2. In this report, the constant C_1 can be determined by the dimensions of the flow meter as $C_1 = 1.78\times10^{-5}$.

Experimental results for two input conditions are shown in Fig. 16 and 17. Input variables for the calculated flow rate, namely, the detected torque T and oil temperature Θ, are shown as functions of time in panel (a) of each figure, while the calculated Q and reference flow Q_{ref} are compared over time in panel (b). The experimental conditions are described below.

- Oil temperature is retained constant at 40 °C: Flow rate is varied by the load valve. Under these conditions, flow rate is proportional to the detected torque.
- Detected torque is retained constant at 0.4 Nm: Oil temperature is decreased from Θ = 50 °C to 37 °C by the heat exchanger.

From these results, although a small deviation occurs as the oil temperature is varied (Fig. 17), the calculated flow rate of the proposed flow meter coincides with the reference flow rate. Thus, the flow rate can be reliably obtained by measuring the torque and oil temperature in the flow meter. The deviation between the calculated and reference flow rates could be reduced by improving the accuracies of the temperature versus viscosity relationship of Eq. 3 and the correction coefficient C_1 of Eq. 5.

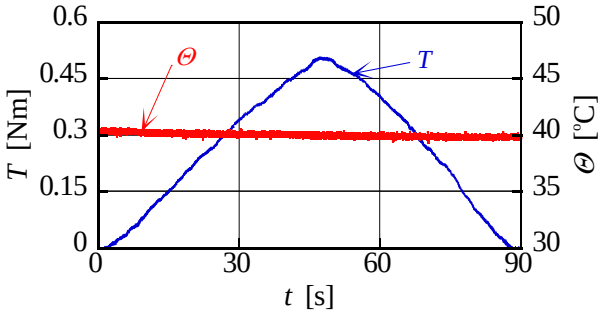

(a) Measured torque and oil temperature

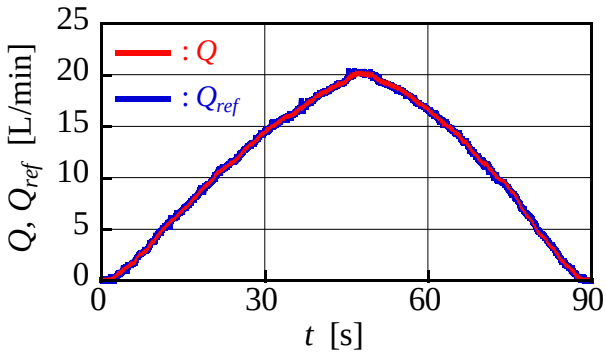

(b) Calculated flow rate Q and reference flow rate Q_{ref}

Fig. 16: *Evaluation of calculated flow rate Q (Experimental condition 1)*

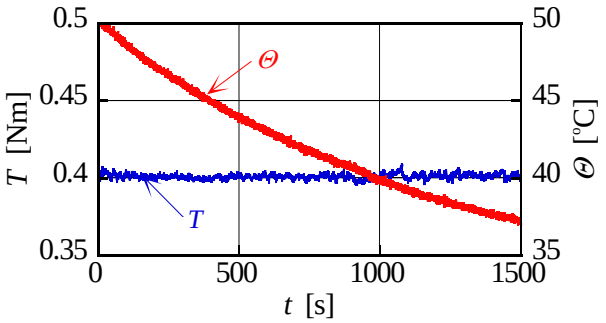

(a) Measured torque and oil temperature

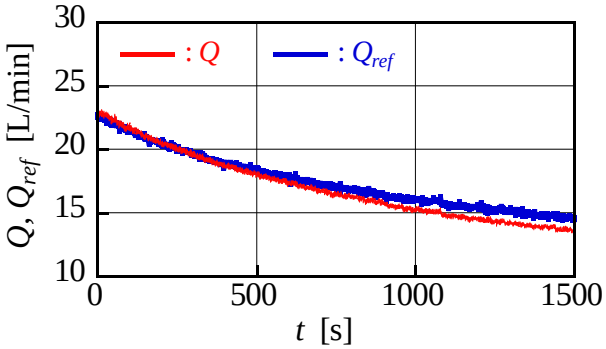

(b) Calculated flow rate Q and reference flow rate Q_{ref}

Fig. 17: *Evaluation of calculated flow rate Q (Experimental condition 2)*

5 Conclusions

In this study, the proposed flow meter was investigated by a series of simulation experiments using the commercial STAR-LT package. The flow behavior of, and pressure distribution inside, a practical configuration of the proposed flow meter were

investigated under various conditions. The obtained CFD results were compared with the predictions of an analytical model on the basis of a two dimensional laminar viscous flow. The simulated and analytical results agreed favorably at low flow rates. At higher flow rates, abrupt contraction flow developed at the connection of the flow meter and circular pipe inlet, with adverse effects on the flow meter performance.

To ameliorate these effects, the configuration of the flow meter and connecting circular pipe was refined. In order to amplify the gain between the flow and torque, the rectangular bar was also redesigned to lie flat on one side. Experimental investigations confirmed that the detected torque versus the reference flow characteristics of the revised meter were linearly and repeatedly obtained for Q = 0 - 20 L/min. In addition, flow rate was calculated from the measured torque and oil temperature data on-line by the digital signal processor. The calculated and reference flow rates agreed favorably under three sets of experimental conditions.

Appendix

A: Analytical Model of Proposed Flow Meter

The following assumptions are made in the theoretical analysis:

- Two dimensional (x-y) laminar viscous flow without flow detachment.
- The y velocity is negligible compared to the x velocity.
- The effect of gravity is negligible.

The dimensions of the analytical flow meter model are shown in Fig. 1. The laminar viscous flow in the inclined clearance is well known theoretically (Watton, 2009). The flow rate in the upstream line left and right of the bar center O are described by Eq. A.1, while that in the downstream line is given by Eq. A.2.

$$\left.\begin{aligned} Q_{L1} &= \frac{b}{3\mu l}\cdot\frac{(h_{Li}h_{Lo})^2}{h_{Li}+h_{Lo}}(P_1-P_{Lo}) \\ Q_{R1} &= \frac{b}{3\mu l}\cdot\frac{(h_{Ri}h_{Ro})^2}{h_{Ri}+h_{Ro}}(P_1-P_{Ro}) \end{aligned}\right\} \tag{A.1}$$

$$\left.\begin{aligned} Q_{L2} &= \frac{b}{3\mu l}\cdot\frac{(h_{Lo}h_{Li})^2}{h_{Lo}+h_{Li}}(P_{Lo}-P_2) \\ Q_{R2} &= \frac{b}{3\mu l}\cdot\frac{(h_{Ro}h_{Ri})^2}{h_{Ro}+h_{Ri}}(P_{Ro}-P_2) \end{aligned}\right\} \tag{A.2}$$

Since $Q_L = Q_{L1} = Q_{L2}$ and $Q_R = Q_{R1} = Q_{R2}$, the following relationship holds.

$$P_{Lo} = P_{Ro} = \frac{P_1+P_2}{2} \tag{A.3}$$

Therefore, the flow rate through the flow meter is

$$Q = Q_L + Q_R = \varepsilon\frac{b(P_1-P_2)}{6\mu l}h_i^3 \tag{A.4}$$

The flow coefficient ε is a function of the non-dimensional clearance $\bar{h} = h_o/h_i$ and the non-dimensional offset $\bar{e} = e/h_i$ as follows.

$$\varepsilon = \frac{(1-\bar{e})^2(\bar{h}-\bar{e})^2}{1+\bar{h}-2\bar{e}} + \frac{(1+\bar{e})^2(\bar{h}+\bar{e})^2}{1+\bar{h}+2\bar{e}} \tag{A.5}$$

The non-dimensional pressure difference $\Delta\bar{P}$ between the left and right side of the bar is described by

$$\Delta\bar{P} = \frac{\mathrm{sign}(\bar{x})}{2}\left\{\frac{\left(\dfrac{\bar{h}+\bar{e}}{\bar{h}+\bar{e}-2\mathrm{sign}(\bar{x})(1-\bar{h})\bar{x}}\right)^2-1}{\left(\dfrac{\bar{h}+\bar{e}}{1+\bar{e}}\right)^2-1} - \frac{\left(\dfrac{\bar{h}-\bar{e}}{\bar{h}-\bar{e}-2\mathrm{sign}(\bar{x})(1-\bar{h})\bar{x}}\right)^2-1}{\left(\dfrac{\bar{h}-\bar{e}}{1-\bar{e}}\right)^2-1}\right\} \tag{A.6}$$

Let T be the torque generated around the bar center O. The non-dimensional torque τ is expressed as

$$\tau = \frac{T}{2bl^2(P_1-P_2)} = \int_0^{1/2}\bar{x}\Delta\bar{P}d\bar{x} \tag{A.7}$$

Hence, the flow rate Q and the torque T are related through the gain factor $\kappa = \tau/\varepsilon$ as follows.

$$\frac{Q}{T} = \frac{h_i^3}{12\mu\kappa l^3} \tag{A.8}$$

B: Analytical Model of Revised Flow Meter

For the revised flow meter, the difference to the original flow meter described in the appendix A appears that the left side of the rectangular bar becomes flat. The right side channel flow rates for both upstream and downstream lines are given by Eq. B.1.

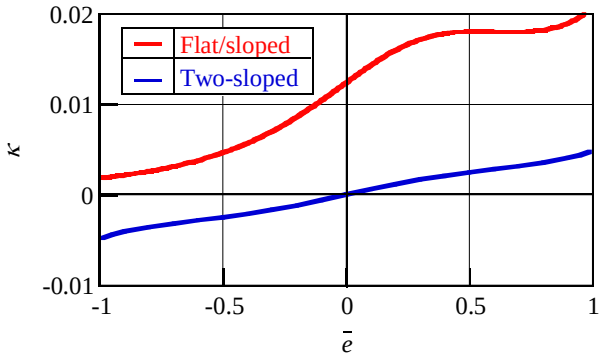

Fig. B.1: *Comparison of gain factor* κ ($\bar{h}$ = 2.0)

The flow of the left side channel, which is a parallel clearance flow between two planes, is given by Eq. B.2.

$$\left.\begin{aligned} Q_{R1} &= \frac{b}{3\mu l}\frac{(h_{Ri}h_{Ro})^2}{h_{Ri}+h_{Ro}}(P_1-P_{Ro}) \\ Q_{R2} &= \frac{b}{3\mu l}\frac{(h_{Ro}h_{Ri})^2}{h_{Ro}+h_{Ri}}(P_{Ro}-P_2) \end{aligned}\right\} \tag{B.1}$$

$$\left.\begin{aligned} Q_{L1} &= \frac{bh_{Li}^3}{6\mu l}(P_1 - P_{Lo}) \\ Q_{L2} &= \frac{bh_{Lo}^3}{6\mu l}(P_{Lo} - P_2) \end{aligned}\right\} \quad \text{(B.2)}$$

The flow rate through the revised flow meter is expressed as

$$Q = Q_L + Q_R = \varepsilon_r \frac{b(P_1 - P_2)}{6\mu l} h_i^3 \quad \text{(B.3)}$$

and the flow coefficient for the revised flow meter ε_r is

$$\varepsilon_r = \frac{(1+\bar{e})^2(\bar{h}+\bar{e})^2}{1+\bar{h}+2\bar{e}} + \frac{(1-\bar{e})^3}{2} \quad \text{(B.4)}$$

The non-dimensional pressure difference $\Delta\bar{P}_r$ is

$$\Delta\bar{P}_r = \frac{\mathrm{sign}(\bar{x})}{2}\left\{\frac{\left(\dfrac{\bar{h}+\bar{e}}{\bar{h}+\bar{e}-2\mathrm{sign}(\bar{x})(1-\bar{h})\bar{x}}\right)^2 - 1}{\left(\dfrac{\bar{h}+\bar{e}}{1+\bar{e}}\right)^2 - 1} - 2\bar{x}\right\} \quad \text{(B.5)}$$

The non-dimensional torque τ_r is obtained as

$$\tau_r = \frac{T}{2bl^2(P_1 - P_2)} = \int_0^{1/2} \bar{x}\Delta\bar{P}_r d\bar{x} \quad \text{(B.6)}$$

The flow rate Q and the torque T are related via the gain factor $\kappa_r = \tau_r / \varepsilon_r$ as follows.

$$\frac{Q}{T} = \frac{h_i^3}{12\mu\kappa_r l^3} \quad \text{(B.7)}$$

The gain factor of the bar with flat/slope geometry is compared with that of the original two-sloped bar in Fig. A.1. This figure plots the shift versus the gain factor κ at the non-dimensional clearance $\bar{h}$ = 2.0. The gain factor of the revised flow meter is almost four times larger than that of the original. It should be noted that the torque of the two-sloped flow meter will be generated in the clockwise direction if the non-dimensional offset is $\bar{e}$ < 0 and its gain factor will be symmetric about the origin.

Nomenclature

a	width of rectangular bar	[mm]
b	height of rectangular bar	[mm]
C_1	constant value	[-]
C_2	correction coefficient κ_{ex}/κ_r	[-]
e	offset distance between the flow line center and bar center	[mm]
$\bar{e}$	non-dimensional offset e/h_i	[-]
h_i	entrance clearance without offset	[mm]
h_o	center clearance without offset	[mm]
h_L	entrance clearance of left side flow channel	[mm]
h_R	entrance clearance of right side flow channel	[mm]
$\bar{h}$	non-dimensional clearance h_o/h_i	[-]
l	length of rectangular bar	[mm]
P_L	pressure of left side flow channel	[Pa]
P_R	pressure of right side flow channel	[Pa]
$\Delta\bar{P}$	non-dimensional pressure difference $(P_L - P_R)/(P_1 - P_2)$	[-]
q	local flow rate	[L/min]
Q	flow rate	[L/min]
T	generated torque	[Nm]
$\bar{x}$	non-dimensional distance x/l	[-]
ε	flow coefficient	[-]
ε_r	flow coefficient for revised flow meter	[-]
κ	gain factor ε / τ	[-]
κ_{ex}	gain factor obtained from experimetnal resutlt	[-]
κ_r	gain factor for revised flow meter ε_r/τ_r	[-]
τ	non-dimensional torque	[-]
τ_r	non-dimensional torque for revised flow meter	[-]
μ	dynamic viscosity of fluid	[Pa·s]

Suffix

1	entrance of flow meter
2	exit of flow meter
i	inlet of bar
o	centre of bar
L	left side
R	right side

References

ASTM D2160-92 1992. Standard Test Method for Thermal Stability of Hydraulic Fluids**.**

Blackburn, J. F. 1953. Lateral Forces on Hydraulic Pistons, *Trans. ASME*, 75. pp. 1175 - 1180**.**

Esser, J. and **Backe, W.** 1994. Development of a New Flow Ripple Sensor for the Measurement of Pump Ripple, *Proc. of Seventh Bath International Fluid Power Workshop; Innovations in Fluid Power*, pp. 262 - 278.

Geißler, G. 1998. Flow Force Coefficient - a Basis for Valve Analysis, *Proc. of Power Transmission and Motion Control '98*, pp. 235 - 250.

Nishiumi, T., **Ichiyanagi, T.** and **Konami, S.** 2004. A Study on the Flowmeter Utilizing Lateral Fluid Force Acted on a Stationary Tapered Body in a Fluid Line, *Transaction of the Japan Fluid Power Systems Society*, 35 - 4, pp. 63 - 69. (in Japanese)

Watton, J. 2009. *Fundamentals of Fluid Power Control*, Cambrigde University Press**.**

Yokota, S., **Kim, DT.** and **Nakano, K.** 1992. An Unsteady Flow Rate Measurement Method Utilizing Dynamic Characteristics Between Pressure and Flow Rate along a Pipeline (A Method Using Pressures at Two Separated Points) , *JSME International Journal (Ser.III)*, 35 - 4, pp. 591 - 597.

Zhao, T., **Kitagawa, A.**, **Kagawa, T.** and **Takenaka, T.** 1987. A Real Time Method of Measuring Unsteady Flow Rate and Velocity Employing Differential Pressure in a Pipe, *JSME International Journal*, 30 - 260, pp. 263 - 270.

Takayoshi Ichiyanagi
Born in Tokyo. He received his doctor degree in Mechanical Engineering from Kanagawa University, Japan in 2001. Since then he works as an assistant professor of mechanical systems engineering at National defense academy of Japan. His research areas are noise reduction of fluid power system, system identification, development of fluid power components.

Takao Nishiumi
Born in 1953 in Tokyo. He is a professor at National Defense Academy of Japan in the Department of Mechanical Systems Engineering. He published the books “Hydraulic Control System” and “Fluid Mechanics for Beginners”, “Hydraulics for Beginners” in Japanese.